Prolyl Isomerase as a Probe of Stability of Slow-Folding Intermediates†

Sudha Veeraraghavan,‡,§ Sofia Rodriguez-Ghidarpour,‡ Christy MacKinnon,‖ William A. McGee,‡ Michael M. Pierce,‡ and Barry T. Nall*,‡

Department of Biochemistry, University of Texas Health Science Center, San Antonio, Texas 78284-7760, and Department of Biology, Incarnate Word College, San Antonio, Texas 78209-6397

Received May 30, 1995; Revised Manuscript Received July 26, 1995⊗

ABSTRACT: Catalysis of slow folding reactions by peptidyl prolyl *cis*−*trans* isomerase (PPI) provides estimates of stabilities of intermediates in folding of normal and mutational variants of yeast iso-2 cytochrome *c*. A two-state model postulating a rapid preequilibration of intermediates with the unfolded protein is employed to calculate the stabilization free energy of the intermediate from the catalytic efficiency (k_{cat}/K_m) of PPI toward slow folding species. Stability measurements have been made for two distinct slow-folding intermediates: the absorbance-detected (I^I_S) and fluorescence-detected (I^{II}_S) intermediates. Mutation-induced changes in the stability of the intermediates and in the activation free energy for slow folding are compared to changes in equilibrium thermodynamic stability. The results show that (1) for iso-2 the absorbance-detected intermediates (I^I_S) are slightly more stable than the fluorescence-detected intermediates (I^{II}_S), (2) most mutations have different effects on equilibrium stability and the stability of the I^I_S or I^{II}_S intermediates, and (3) for both slow folding reactions the mutation-induced changes in the activation free energy are small compared to the magnitude of the activation free energy barrier. Differential effects of mutations on equilibrium stability and the stability of intermediates provides a means of assessing the sequence-encoded structural specificity for folding. Mutations with different effects on intermediate stability and equilibrium stability change the encoded folding information and may alter folding pathways and/or lead to different three-dimensional structures. Identification of mutations which stabilize a folding intermediate relative to the native conformation provides an empirical approach to the design of thermodynamically stable forms of folding intermediates.

Much of the kinetic complexity observed in protein refolding reactions arises from a heterogeneous unfolded state containing both fast- and slow-folding forms of the unfolded protein (Garel & Baldwin, 1973). For a number of small proteins the slow-folding species are known to be produced by proline *cis*−*trans* isomerization in the fully unfolded protein (Brandts et al., 1975; Kelley & Richards, 1987; Kiefhaber et al., 1990; Schmid & Baldwin, 1978; Wood et al., 1988b). Thus, it is not surprising that the enzyme peptidyl prolyl *cis*−*trans* isomerase (PPI)[1] catalyzes many slow protein folding reactions (Bachinger, 1987; Fischer & Bang, 1985; Lang et al., 1987; Schmid et al., 1993; Schonbrunner et al., 1991) and allows identification of kinetic phases that arise from proline isomerization. PPI catalysis of protein folding is efficient, but much less efficient than catalysis of *cis*−*trans* isomerization in unstructured model peptides (Schmid, 1993). This suggests that structure in folding intermediates modulates access of PPI to target proline residues within folding intermediates, and that quantitative measurements of PPI catalysis of folding provides a means of detecting and characterizing structure in slow-folding intermediates. In support of this hypothesis, we have recently reported (Veeraraghavan & Nall, 1994) that PPI catalysis of folding of iso-2 cytochrome *c* is at least 1000-fold less efficient than catalysis of proline isomerization in unstructured model peptides, but that the efficiency of PPI catalysis of slow protein folding is enhanced by structure disrupting agents such as protein denaturants (guanidine hydrochloride) and site-specific mutagenesis of iso-2.

Yeast iso-2 cytochrome *c* is a small globular protein with a fully reversible unfolding transition. Refolding of completely unfolded iso-2 to a fully folded state involves at least one fast folding phase detected by changes in either absorbance or fluorescence that accounts for 70-85% of the kinetically observed signal change. Two different slow-folding reactions are detected by different optical probes, absorbance and fluorescence (Nall, 1983; Nall & Landers,

† Supported by grants from the National Institute of General Medical Sciences (GM32980), the National Center for Research Resources (RR05043), and Robert A. Welch Foundation (AQ838).

* Address correspondence to this author at the Department of Biochemistry, University of Texas Health Science Center, 7703 Floyd Curl Dr., San Antonio, TX 78284-7760. E-mail: nall@bioc01.uthscsa.edu.

‡ University of Texas Health Science Center.

§Present address: Department of Biochemistry, Tufts University School of Medicine, 136 Harrison Ave., Boston MA, 02111.

‖Incarnate Word College.

⊗ Abstract published in *Advance ACS Abstracts,* September 15, 1995.

[1] Abbreviations: PPI, peptidyl prolyl *cis*−*trans* isomerase, also known as human cyclophilin (hCyp), a cyclosporin A binding protein; CsA, cyclosporin A; iso-2, iso-2 cytochrome *c* from the yeast *Saccharomyces cerevisiae*; XnY iso-2, variant forms of iso-2 where *n* is the sequence position (mammalian cytochrome *c* numbering) and X and Y are normal and mutant amino acids occurring at position *n*, for example, P25G iso-2 is iso-2 in which proline 25 is replaced by glycine; succinyl-AAPF-*p*-nitroanilide, tetrapeptide substrate used in the determination of the specific activity of PPI (succinyl-Ala-Ala-Pro-Phe-*p*-nitroanilide); DTT, dithiothreitol; EDTA, ethylenediaminetetraacetic acid; SDS, sodium dodecyl sulfate; Gdn·HCl, guanidine hydrochloride; SDS−PAGE, polyacrylamide gel electrophoresis in the presence of sodium dodecyl sulfate; k_{cat}/K_m, catalytic efficiency of PPI; $(k_{cat}/K_m)_{pep}$, catalytic efficiency of PPI toward the peptide substrate; $(k_{cat}/K_m)_{prot}$, catalytic efficiency of PPI toward protein substrate (cytochrome *c*); $(k_{cat}/K_m)_{rel}$, catalytic efficiency of PPI toward the protein substrate relative to peptide substrate.

0006-2960/95/0434-12892$09.00/0

1981), and, under appropriate conditions, both phases are catalyzed by PPI showing that the slow reactions involve prolyl *cis*−*trans* isomerization (Veeraraghavan & Nall, 1994). The rates of the two slow-folding phases differ depending on the final refolding conditions, with the fluorescence-detected phase being 3−20-fold faster than the absorbance-detected phase. While the mechanisms of coupling of the different slow kinetic phases to distinct optical probes are not known, it is likely that the different spectral properties result from differences in structure within the folding intermediates. The hypothesis that different prolines are involved in the different slow phases is supported by double-jump measurements (Osterhout & Nall, 1985) of the rates of formation of the slow refolding species. The double-jump experiments show that the absorbance-detected slow refolding species are generated within the unfolded protein on a distinctly different time scale than the fluorescence-detected slow-folding species. Furthermore, folding of P76G iso-2 lacks the absorbance-detected slow phase, suggesting that the absorbance-detected intermediates are generated by isomerization of Pro76 (Wood et al., 1988b). The fluorescence-detected slow-folding intermediates are probably generated by isomerization of two or more of the remaining prolines: Pro71, Pro30, Pro25, or Pro-1. The identity of the prolines that generate the fluorescence-detected slow-refolding species is uncertain.

Here, we develop a means of measuring the stability of slow-folding intermediates. The approach assumes that slow-folding species preequilibrate between PPI-accessible and PPI-inaccessible forms, so that the catalytic efficiency (k_{cat}/K_m) of PPI toward slow-folding species is a measure of the fraction of those species in the PPI-accessible form. The formalism used to relate measured values of k_{cat}/K_m to the stability of the intermediates is borrowed from that developed to interpret the Gdn·HCl dependence of hydrogen exchange (HX) from folded proteins (Mayo & Baldwin, 1993). Assuming a linear extrapolation model (Pace, 1986), the dependence of catalysis on the concentration of a structure destabilizing agent, Gdn·HCl, gives an estimate of $\Delta G^*_{I(H_2O)}$ (or $\Delta G^*_{II(H_2O)}$), the free energy of stabilization of the intermediates in the absence of denaturant, and also the dependence of the free energy on the concentration of denaturing agent: $m_I = d\Delta G_I/d[Gdn{\cdot}HCl]$ (or $m_{II} = d\Delta G_{II}/d[Gdn{\cdot}HCl]$). The formalism is used to assess the effects of several site-directed mutations on the stability of the intermediates. The mutational sites have been selected to span a large part of the amino acid sequence in order to obtain information on the location of structured regions within folding intermediates. Together with results reported previously for iso-2 and P25G iso-2 (Veeraraghavan & Nall, 1994), six different locations are probed: sites 25, 30, 33, 52, 75, and 76. In most but not all cases the mutations decrease the stability of the native protein. The results show that there is a surprisingly good correlation between the effects of the mutations on the stability of slow folding intermediates, $\Delta G^*_{I(H_2O)}$ (or $\Delta G^*_{II(H_2O)}$), and the dependence of intermediate stability on the Gdn·HCl concentration, m_I (or m_{II}). There is also a correlation between the effects of mutations on the equilibrium stability, $\Delta G°_U$, and the dependence of the equilibrium stability on the concentration of Gdn·HCl, $m = d\Delta G_U/d[Gdn{\cdot}HCl]$. However, the functional dependence of the stability of slow-folding intermediates on m_I or m_{II} and equilibrium stability on m is different, indicating that slow-folding intermediates differ from the native protein in the manner in which mutational perturbations are accommodated.

We suggest that the differences between folding intermediates and fully folded proteins in susceptibility to mutational perturbation reflect changes in structural specificity encoded into the amino acid sequence. Thus, the formalism presented here provides an experimental means of addressing the problem posed by Lattman and Rose (1993) of distinguishing between mutational effects on thermodynamic stability vs structural specificity. Some mutational changes preferentially enhance intermediate stability compared to the stability of the native protein. Changes in amino acid sequence that result in an intermediate that is more stable than the native protein encode a new thermodynamically stable three-dimensional structure, that of the intermediate. While such structures may be "native-like", they differ from the native structure in certain critical features such as having a *thermodynamic* preference for nonnative *cis* or *trans* isomeric configurations about specific proline imide bonds. In contrast, mutations which enhance the stability of the native protein over that of the intermediate favor retention of the normal folding pathway and formation of the same (native) three-dimensional structure.

MATERIALS AND METHODS

Protein Isolation and Characterization. Normal and mutant forms of iso-2 cytochrome *c* from *Saccharomyces cerevisiae* were grown and isolated as described previously (Nall & Landers, 1981; Wood et al., 1988a; Zuniga & Nall, 1983). After lyophilization the purified proteins were stored at −70 °C until needed for sample preparation. Methods of purifying and characterizing PPI have been described in detail previously (Veeraraghavan & Nall, 1994).

Site-Directed Mutagenesis. Construction of iso-2 mutational variants was carried out as described (Guillemette et al., 1994; Inglis et al., 1991) for site-directed mutagenesis and expression of the yeast iso-1 cytochrome *c* gene. The mutagenesis experiments were performed on the plasmid pEMBLYe30-CYC7, which was constructed by inserting a 0.6 kb *Sau*3A fragment of DNA containing the structural gene (CYC7) for the iso-2 isozyme of yeast cytochrome *c* (Montgomery et al., 1980) into the *Bam*HI site of the yeast *Escherichia coli* phagemid pEMBLYe30. The pEMBLYe30-CYC7 phagemid has the advantage that the same cloning vector can be used to prepare double-stranded plasmid DNA in *E. coli* to express the iso-2 cytochrome *c* protein in the yeast and to prepare single-strand template DNA for site-directed mutagenesis and DNA sequencing. Mutant genes were identified by dideoxy-DNA sequencing. The primary structures of the purified mutant proteins were verified by electrospray ion mass spectrometry.

Equilibrium Unfolding Free Energies. Gdn·HCl-induced equilibrium unfolding transitions were measured by fluorescence emission at 350 nm (excitation at 280 or 285 nm) in 0.1 M sodium phosphate, pH 6, at 20 °C. Samples used to measure the equilibrium unfolding transition curve were prepared in two ways: (1) by adding Gdn·HCl to a solution of folded protein and (2) by diluting Gdn·HCl from a solution of unfolded protein. Samples prepared in both ways gave the same transition showing that equilibrium had been attained (Nall & Landers, 1981). The data were analyzed

using the linear extrapolation model (Pace, 1986) as described by Santoro and Bolen (1988). Two parameters are obtained from the analysis: $\Delta G°_U$, the extrapolated free energy of unfolding in the absence of denaturant, and m, the denaturant dependence of the unfolding free energy.

Differential scanning calorimetry measurements of protein stability were carried out in 0.1 M sodium phosphate buffer, pH 6.0. The transitional enthalpy, ΔH_m, and transition midpoint, T_m, were determined by fitting the temperature dependence of the molar heat capacity, $C_P(T)$, to a two-state model with an adjustable $\Delta H^{vH}/\Delta H^{cal}$ value and a temperature dependent ΔC_P as described previously (Liggins et al., 1994). The values for $\Delta G°_U$ (H_2O) at 20 °C were calculated from the T_m and the transitional enthalpy, ΔH_m, as described by Schellman (Becktel & Schellman, 1987; Schellman, 1987b) using ΔC_P = 1.58 kcal mol^{-1} (W. A. McGee, unpublished data) (Liggins et al., 1994).

Kinetic Measurements. The procedures for measuring the rates of absorbance-detected and fluorescence-detected slow folding in the presence and absence of PPI have been described previously (Veeraraghavan & Nall, 1994). Digitized kinetic traces were analyzed using the Bio-Kine software (Molecular Kinetics, Inc., Pullman, WA). Apparent first-order rate constants (k_{obs}) were obtained by nonlinear least-squares fits of the data to

$$A_\infty - A(t) = [A_\infty - A_o] \exp(-k_{obs}t) \quad (1)$$

where, A_o is absorbance or fluorescence at $t = 0$, A_∞ the final absorbance or fluorescence, and $A(t)$ the measurement at time t.

The specific activity, $(k_{cat}/K_m)_{pep}$, for the peptide substrate, suc-AAPF-*p*-nitroanilide, was determined according to Harrison and Stein (1990) using

$$(k_{cat}/K_m)_{pep} = (k_{obs} - k_f)/[PPI] \quad (2)$$

where k_{obs} is the observed first-order rate constant (measured by absorbance at 390 nm), k_f is the uncatalyzed rate, and [PPI] is the concentration of PPI used in the assay. The catalytic efficiency for the protein substrate, $(k_{cat}/K_m)_{prot}$, was determined in the same way using eq 2 or from the slope of a plot of k_{obs} vs [PPI]. The relative catalytic efficiency, $(k_{cat}/K_m)_{rel}$, is given by

$$(k_{cat}/K_m)_{rel} = (k_{cat}/K_m)_{prot}/(k_{cat}/K_m)_{pep} \quad (3)$$

which normalizes the observed $(k_{cat}/K_m)_{prot}$ values and corrects for loss of enzyme activity in the presence of Gdn·HCl.

The sensitivity of the activity assay depends on a variety of factors, one being the difference between the uncatalyzed rate (k_f) and the catalyzed rate (k_{obs}). Within the limitations of enzyme and substrate solubility and the time resolution of the kinetic instrumentation, the difference, $k_{obs} - k_f$, can be increased by increasing the PPI concentration (see eq 2). In practice this has allowed the sensitivity of the assay to be maintained within about ±0.1 (k_{cat}/K_m) over the 0−0.7 M Gdn·HCl concentration range for both peptide and protein substrates.

RESULTS

Equilibrium Thermodynamic Stability Measured by Gdn·HCl-Induced Unfolding and by Scanning Calorimetry.

Table 1: Equilibrium Thermodynamic Stability of Iso-2 and Mutational Variants of Iso-2[a]

protein	$\Delta G°_{U(H_2O)}$[b,c] (kcal mol^{-1}) calorimetry[b]	Gdn·HCl unfolding[c]	m[c] (kcal mol^{-1} M^{-1})	C_m[c] (M^{-1})	T_m[b] (°C)
iso-2	4.2 ± 0.2	4.9 ± 0.3	3.2 ± 0.2	1.5	55.4
N52I iso-2	6.6 ± 0.2	8.4 ± 0.5	3.9 ± 0.2	2.2	64.6
P30A, N52I iso-2	4.5 ± 0.1	4.7 ± 0.4	3.7 ± 0.3	1.3	48.0
H33N iso-2	3.4 ± 0.1	3.6 ± 0.3	2.9 ± 0.2	1.2	50.0
P76G iso-2	1.3 ± 0.2	3.8 ± 0.3	3.1 ± 0.2	1.2	51.4
P25G iso-2	4.7 ± 0.1	4.1 ± 0.2	2.9 ± 0.2	1.4	54.3
I75M, N52I iso-2	3.9 ● 0.2	6.0 ± 0.4	3.4 ± 0.2	1.8	60.0

[a] Values of $\Delta G°_{U(H_2O)}$ are for 0.1 M sodium phosphate, pH 6.0, and a reference temperature of 20 °C. [b] $\Delta G°_{U(H_2O)}$ at 20 °C and the thermal transition midpoint, T_m, determined by scanning calorimetry. $\Delta G°_{U(H_2O)}$ at 20 °C is calculated from the T_m and the transitional enthalpy, ΔH_m, as described by Schellman (Becktel & Schellman, 1987; Schellman, 1987b) using ΔC_P = 1.58 ± 0.07 kcal mol^{-1} (W. A. McGee, unpublished data) (Liggins et al., 1994). Errors in $\Delta G°_{U(H_2O)}$ are estimated from those propagated from ΔH_m and ΔC_P assuming that errors in T_m can be neglected. [c] For the Gdn·HCl-induced unfolding transitions monitored by fluorescence, values for $\Delta G°_{U(H_2O)}$ and m were obtained for the linear extrapolation model (Pace, 1986) by fitting the fluorescence data as described by Santoro and Bolen (1988). In fitting the equilibrium unfolding data, the pretransition slope was fixed at zero, since for many of the less stable mutant proteins there is very little pretransition baseline. If, in fitting the data, the value of the pretransition slope is allowed to float, the statistical errors in the slope are usually greater than the value of the slope. C_m, the midpoint of the Gdn·HCl-induced unfolding transition, is obtained from $C_m = \Delta G°_{U(H_2O)}/m$. The cytochrome c concentrations were 1−5 μM. Errors in the parameters are statistical errors obtained from fitting the data to the model.

Two methods have been used to measure the equilibrium thermodynamic stability of iso-2 and mutant variants of iso-2. Gdn·HCl-induced equilibrium unfolding transitions have been analyzed using the linear extrapolation model to obtain unfolding free energies in the absence of denaturant (Pace, 1986; Santoro & Bolen, 1988). Stability has also been calculated from temperature-induced transitions in which the temperature dependence of the heat capacity is measured by scanning microcalorimetry. The calorimetry experiments give three parameters: T_m, the midpoint of the temperature-induced transition, ΔH_m, the transitional enthalpy at $T = T_m$, and ΔC_P, the transitional change in heat capacity. Using standard thermodynamic relationships (Schellman, 1987b), these three parameters are used to calculate the temperature dependence of the equilibrium unfolding free energy in the absence of Gdn·HCl. The results of both kinds of stability measurements are listed in Table 1.

A Model Relating PPI Catalysis of Folding to the Stability of Intermediates. The unfolded state of iso-2 is a heterogeneous mixture of three slowly interconverting unfolded species: the fast folding U_F species, absorbance-detected slow folding U^I_S species, and fluorescence-detected slow folding U^{II}_S species (Osterhout & Nall, 1985). At equilibrium in the unfolded state the populations of each of these species are estimated to be 73% U_F, 19% U^IS, and 8% U^{II}_S. Formation of the U_S species is known to result from isomerization of proline imide bonds to nonnative *cis* isomeric forms in the unfolded protein (Veeraraghavan & Nall, 1994). Interconversion between the three forms of unfolded species is slow compared to fast folding and formation of partially folded I_S species. Thus, when unfolded protein is returned to conditions where the native protein is

stable, refolding proceeds by one fast pathway (eq 4A) and two slow (eq 4BC) pathways:

$$U_F \xrightarrow{\text{fast}} N \quad (4A)$$

$$U^I_S \xleftrightarrow{\text{fast}} I^I_S \xrightarrow{\text{very slow}} N \quad (4B)$$

$$U^{II}_S \xleftrightarrow{\text{fast}} I^{II}_S \xrightarrow{\text{slow}} N \quad (4C)$$

After completion of the fast kinetic phase in folding (eq 4A), the remaining protein refolds by the absorbance-detected (eq 4B) and the fluorescence-detected (eq 4C) slow-folding pathways. Since the following discussion applies equally well to eqs 4B and 4C, the superscripts (e.g., I, II) will be dropped. The U_S species are assumed to be at least partially unstructured so that the critical proline (or prolines) is accessible to catalysis by PPI, while the I_S species are highly structured so that access of PPI to the critical proline (or prolines) is blocked. The preequilibrium between the U_S and I_S species is much faster than subsequent very slow (eq 4B) or slow (eq 4C) reactions which involve proline *cis*–*trans* isomerization (Veeraraghavan & Nall, 1994). Since only U_S species are competent PPI substrates, shifts in the $U_S \leftrightarrow I_S$ preequilibrium alter the catalytic efficiency of PPI toward the total slow folding species, ($U_S + I_S$). For example, increases in the Gdn·HCl concentration in the final refolding conditions are expected to shift the preequilibrium slightly toward the PPI-accessible U_S species and, thus, increase the catalytic efficiency of PPI toward the total slow-folding species. Note that eq 4 describes only uncatalyzed slow folding and does not explicitly include the PPI-catalyzed $U_S \rightarrow N$ path, the rate of which depends on the PPI concentration. Catalyzed folding involves conversion of the PPI-accessible U_S species to U_F species with a rate constant of $(k_{cat}/K_m)_{prot}$[PPI]. The U_F species, in turn, are rapidly converted to the native protein. For complete refolding the $U_S \rightarrow U_F$ reaction is assumed to be rate limiting, so the overall rate of formation of the native protein, N, is

$$U_S \xrightarrow{(k_{cat}/K_m)_{prot}[PPI]} N \quad (5)$$

The first-order rate constant for the catalyzed reaction is $(k_{cat}/K_m)_{prot}$ [PPI], so the experimentally observed first-order rate constant, including both the catalyzed ($U_S \rightarrow N$) and the uncatalyzed ($I_S \rightarrow N$) paths, is

$$k_{obs} = k_f + (k_{cat}/K_m)_{prot}[PPI] \quad (6)$$

where k_f is the apparent rate constant of the uncatalyzed $I_S \rightarrow N$ reaction, and $(k_{cat}/K_m)_{prot}$ [PPI] is the apparent rate constant for the catalyzed $U_S \rightarrow N$ reaction. Thus, catalysis will be observed experimentally only when the PPI concentration is sufficiently high that the second term in eq 6, $(k_{cat}/K_m)_{prot}$ [PPI], is comparable to or larger than the first term, k_f. Equation 6 is the analog of eq 2 when folding intermediates rather than unstructured peptides are the substrate for PPI catalysis.

The mechanisms given in eqs 4 and 5 provide a relationship between PPI catalysis of proline isomerization in unstructured peptides and PPI catalysis of slow protein folding reactions. The fraction of the total slow folding species accessible to PPI catalysis is given by $f_u = U_S/(U_S + I_S)$. f_u is assumed to be equal to an experimental quantity, $(k_{cat}/K_m)_{rel}$, given in eq 3. Letting $f_u = (k_{cat}/K_m)_{rel}$ is equivalent to assuming that PPI catalysis of *cis*–*trans* isomerization in a model peptide is equal in efficiency to PPI catalysis of proline isomerization in the PPI-accessible U_S species. The free energy change for unfolding the structured I_S species to the PPI-accessible U_S species can be obtained from the experimental quantity, $f_u = (k_{cat}/K_m)_{rel}$, using

$$\Delta G(\text{Gdn}) = -RT \ln[f_u/(1 - f_u)] \quad (7)$$

The free energy is for a preequilibrium between structured and unstructured slow-folding species all of which will eventually fold to the native state, N. The relationship given in eq 7 exists for both the absorbance-detected and the fluorescence-detected slow-folding intermediates. When it is necessary to distinguish between the two type of intermediates, the free energy of stabilization of the absorbance-detected slow folding intermediates (eq 4B) are denoted ΔG_I, and the free energy of stabilization of the fluorescence-detected slow folding intermediates (eq 4C) are denoted ΔG_{II}.

The linear extrapolation model (Pace, 1986) can be used to describe the Gdn·HCl dependence of the free energy of unfolding of the I_S species. This model assumes that the free energy depends on Gdn·HCl concentration as described in

$$\Delta G(\text{Gdn}) = \Delta G^*(H_2O) - m_{I,II}[\text{Gdn·HCl}] \quad (8)$$

$\Delta G^*_{(H_2O)}$ is the standard state free energy of unfolding for the I_S species in the absence of Gdn·HCl, and $m_{I,II}$ is the dependence of the free energy on the Gdn·HCl concentration for the I_S species. Equation 7 is used to calculate ΔG_I (or ΔG_{II}) from the measured $(k_{cat}/K_m)_{rel}$ at the final Gdn·HCl concentration, while eq 8 gives $\Delta G^*_{I(H_2O)}$ (or $\Delta G^*_{II(H_2O)}$) and m_I (or m_{II}) as the intercept and slope, respectively, of plots of ΔG_I (or ΔG_{II}) vs Gdn·HCl concentration.

Guanidine Hydrochloride Dependence of Stability of Slow-Folding Intermediates. Figure 1A shows the stability of the absorbance-detected I^I_S species (ΔG_I) and Figure 1B the stability of the fluorescence-detected I^{II}_S species (ΔG_{II}) for iso-2 at various Gdn·HCl concentrations. The free energies ($\Delta G_{I(\text{Gdn·HCl})}$ or $\Delta G_{II(\text{Gdn·HCl})}$) are calculated for different Gdn·HCl concentrations using eq 7, and the results are plotted as a function of the Gdn·HCl concentration. Least-squares fits of the plots of ΔG_I (or ΔG_{II}) vs [Gdn·HCl] to eq 8 are in good agreement with the predicted linear dependence of ΔG_I (or ΔG_{II}) on Gdn·HCl concentration. According to eq 8 the *Y*-axis intercept of these plots gives $\Delta G^*_{I(H_2O)}$ (or $\Delta G^*_{II(H_2O)}$) , the stability of the intermediate in the absence of Gdn·HCl, and the slope is m_I (or m_{II}), the Gdn·HCl dependence of the stability of the intermediate (e.g., $m_I = d\Delta G_I/d[\text{Gdn·HCl}]$). Note that the free energies plotted in Figure 1 indicate that a very small fraction of the refolding protein is in the PPI-accessible state ($f_u \sim 0.001-0.01$; see eq 7). Measurements of such small amounts of PPI-accessible protein (f_u) and the conversion of the f_u values to standard free energies (eqs 7 and 8) must be carried out with care. Two factors partially compensate for the difficulties associated with using such small values of f_u to obtain the standard free energies in the absence of denaturant. First, the catalytic efficiency of PPI toward unstructured peptides is very high ($k_{cat}/K_m \sim 10^7\ M^{-1}\ s^{-1}$), and thus measurements are possible at very low concentrations of the PPI-accessible species. Second, the method of directly measuring f_u [as

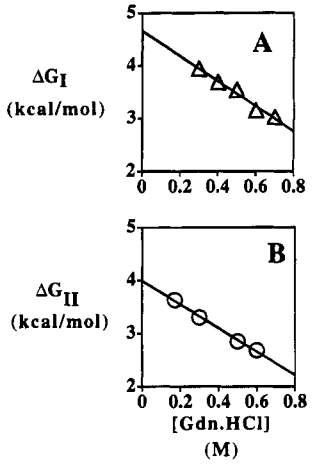

FIGURE 1: Stability of the absorbance-detected (A) and fluorescence-detected (B) slow-folding intermediates of normal iso-2 cytochrome *c* as a function of the concentration of guanidine hydrochloride in the final refolding conditions. In panel A ΔG_I, the apparent free energy of unfolding for the absorbance-detected intermediates (I^I_S), is plotted as a function of the final Gdn·HCl concentration. Panel B gives ΔG_{II}, the apparent free energy of unfolding for the fluorescence-detected intermediates (I^{II}_S), as a function of the final Gdn·HCl concentration. The apparent free energies of unfolding for the intermediates are calculated as described in Materials and Methods (eq 7) from measurements of the catalytic efficiency (k_{cat}/K_m) of PPI for the respective slow-folding intermediates. Measurements of PPI catalysis of slow folding were carried out by unfolding iso-2 in 3 or 3.9 M Gdn·HCl, pH 6.3, 20 °C, and initiating refolding by adding PPI and diluting with sodium phosphate buffer such that the final refolding conditions were 5 μM PPI, 20 μM iso-2, and 0.1 M sodium phosphate, pH 6.0, 20 °C. The solid lines are least-squares fits of the data where the negative of the slope ($m_I = d\Delta G_I/d[\text{Gdn·HCl}]$ or $m_{II} = d\Delta G_{II}/d[\text{Gdn·HCl}]$) is the denaturant dependence of the stability of the intermediates, and the intercept ($\Delta G^*_{I(H_2O)}$, or $\Delta G^*_{II(H_2O)}$), gives the stability of the intermediate in the absence of denaturant (eq 8). For panel A, the absorbance-detected intermediates, I^I_S, $m_I = 2.4 \pm 0.2$ kcal mol^{-1} M^{-1} and $\Delta G^*_{I(H_2O)} = 4.7 \pm 0.1$ kcal mol^{-1}. For panel B the fluorescence-detected intermediates, I^{II}_S, $m_{II} = 2.2 \pm 0.1$ kcal mol^{-1} M^{-1} and $\Delta G^*_{II(H_2O)} = 3.99 \pm 0.04$ kcal mol^{-1}. For both panels A and B the free energy plotted for each Gdn·HCl concentration is an average of 3−7 individual measurements.

the quantity $(k_{cat}/K_m)_{rel}$] below the unfolding transition zone avoids the problems associated with long extrapolations of f_u to zero denaturant concentration. Traditional methods of measuring standard free energies from (equilibrium) measurements of f_u made within the transition zone require long extrapolations which can result in large systematic errors in the standard free energy change. Measurements of the Gdn·HCl dependence of PPI catalysis of absorbance-detected and fluorescence-detected slow folding have also been carried out for several mutant proteins, and the data fit to eq 8. Table 2 lists the parameters describing the stability of the absorbance-detected I^I_S species for iso-2 and mutant variants of iso-2. Table 3 lists the stability parameters for the fluorescence-detected I^{II}_S species for the same proteins.

Effects of Mutations on Activation Free Energies for Slow Folding. Eyring theory of absolute reactions rates (Glasstone et al., 1941) can be used to describe the effects of mutations on the transition state for slow folding. The time constant for the absorbance-detected slow phase in folding is denoted as τ_{1a}, and the time constant for the fluorescence-detected slow phase is τ_{1b} (Nall et al., 1988; Osterhout & Nall, 1985). For refolding ending below the equilibrium unfolding transition zone, the uncatalyzed rate (k_f) for absorbance-detected slow folding is $1/\tau_{1a}$, and for fluorescence-detected slow folding the uncatalyzed rate is $1/\tau_{1b}$. The rates for the absorbance-detected ($I^I_S \rightarrow N$) and fluorescence-detected ($I^{II}_S \rightarrow N$) slow-folding reactions for iso-2 and mutant variants of iso-2 have been extrapolated to standard conditions (20 °C, 0.1 M sodium phosphate, pH 6, 0 M Gdn·HCl) and are listed in Tables 4 and 5. Activation free energies, $\Delta G^{\ddagger}_I$ and $\Delta G^{\ddagger}_{II}$, calculated for the two $I_S \rightarrow N$ reactions using Eyring theory, and the mutation-induced changes in activation free energies, $\Delta\Delta G^{\ddagger}_I$ and $\Delta\Delta G^{\ddagger}_{II}$, are also listed in the tables. The mutation-induced changes in activation free energy are small (<3%) compared to the total activation free energy barrier.

Table 2: Stability of Absorbance-Detected Slow-Folding Intermediates of Iso-2 and Mutational Variants of Iso-2[a]

protein	$\Delta G^*_{I(H_2O)}$ (kcal mol^{-1})	m_I (kcal mol^{-1} M^{-1})	C_{Im} (M^{-1})	r	$\Delta\Delta G^*_I$ (kcal mol^{-1})[c]
iso-2	4.7 ± 0.1	2.4 ± 0.2	2.0 ± 0.2	0.988	(0)
N52I iso-2	4.26 ± 0.04	2.0 ± 0.1	2.2 ± 0.1	0.999	−0.4 ± 0.1
P30A, N52I iso-2	4.5 ± 0.2	2.7 ± 0.5	1.7 ± 0.3	0.952	+0.2 ± 0.2
H33N iso-2	4.0 ± 0.1	2.1 ± 0.2	1.9 ± 0.2	0.983	-0.7 ± 0.1
P76G iso-2[b]	*b*	*b*	*b*	*b*	*b*
P25G iso-2	4.0 ± 0.4	0.9 ±0.7	4.3 ± 3.4	0.43	−0.7 ± 0.4
I75M, N52I iso-2	6.7 ± 0.7	6.2 ± 1.4	1.1 ± 0.3	0.930	+2.4 ± 0.7

[a] Values for $\Delta G^*_{I(H_2O)}$ and m_I are obtained as the intercept and the negative of the slope, respectively, of least-squares fits to plots of ΔG_I versus Gdn·HCl concentration (e.g., Figure 1 A). Each plot was obtained from measurements of ΔG_I at three to five Gdn·HCl concentrations. Three to seven individual measurements were made at each Gdn·HCl concentration. C_{Im}, the midpoint of the Gdn·HCl-induced unfolding transition for $I^I_S \leftrightarrow U^I_S$, is obtained from $C_{Im} = \Delta G^*_{I(H_2O)}/m_I$. The linear correlation coefficients, r, of the fit of the data to a straight line are given in the next to last column. [b] Values are not listed for P76G iso-2, since the absorbance-detected slow phase is not detected in folding of this protein (Wood et al., 1988b). [c] The free energy differences are defined as $\Delta\Delta G^*_I = \Delta G^*_{I(\text{iso-2 mutant "i"})} - \Delta G^*_{I(ref)}$, $\Delta G^*_{I(ref)} = \Delta G^*_{I(iso\text{-}2)}$ for all single mutants, while $\Delta G^*_{I(ref)} = \Delta G^*_{I(N52I\ iso\text{-}2)}$ for double mutants containing the N52I stability-enhancing mutation.

DISCUSSION

Folding Intermediates and Fully Folded Proteins: Relationships between Stability and the Cooperativity of Gdn·HCl-Induced Unfolding Transitions. For the linear extrapolation model, the parameter m (m_I or m_{II}, for intermediates) is related to the difference in the preferential interaction of the unfolded protein with denaturant compared to the interaction of the folded protein with denaturant (Pace, 1990a,b; Schellman, 1978, 1987a,b). This theoretical interpretation of the m values suggests that a relationship may exist between the free energies and the m values (or $m_{I,II}$ values) for protein conformations stabilized by a common mechanism. For example, a linear relationship has been shown to exist between the free energies and m values that describe the Gdn·HCl dependence of hydrogen−deuterium exchange (HX) of some classes of amide protons from ribonuclease A (Mayo & Baldwin, 1993).

For the equilibrium Gdn·HCl-induced unfolding transitions for iso-2 and mutational variants of iso-2, Figure 2 shows that there is a correlation ($r = 0.82$) between the standard free energies of unfolding and the m values for the transitions. Figure 2 also shows that a significantly different linear correlation exists between $\Delta G^*_{(H_2O)}$ and $m_{I,II}$ for the slow

Table 3: Stability of Fluorescence-Detected Slow-Folding Intermediates of Iso-2 and Mutational Variants of Iso-2[a]

protein	$\Delta G^*_{II(H_2O)}$ (kcal mol^{-1})	m_{II} (kcal mol^{-1} M^{-1})	C_{IIm} (M^{-1})	r	$\Delta\Delta G^*_{II}$ (kcal mol^{-1})[b]
iso-2	3.99 ± 0.04	2.2 ± 0.1	1.8 ± 0.1	0.998	(0)
N52I iso-2	4.6 ± 0.4	3.1 ± 0.7	1.5 ± 0.4	0.934	0.6 ± 0.4
P30A, N52I iso-2	3.7 ± 0.2	1.7 ± 0.4	2.2 ± 0.5	0.925	-0.9 ± 0.4
H33N iso-2	4.5 ± 0.4	2.9 ± 0.9	1.5 ± 0.5	0.924	0.5 ± 0.4
P76G iso-2	4.5 ± 0.1	2.5 ± 0.4	1.8 ± 0.3	0.971	0.5 ± 0.1
P25G iso-2	3.1 ± 0.1	0.7 ± 0.2	4.1 ± 1.2	0.892	-0.9 ± 0.1
I75M, N52I iso-2	3.8 ± 0.1	1.5 ± 0.4	2.5 ± 0.5	0.904	-0.8 ± 0.4

[a] Values for $\Delta G^*_{II(H_2O)}$ and m_{II} are obtained as the intercept and the negative of the slope, respectively, of least-squares fits to plots of ΔG_{II} versus Gdn·HCl concentration (e.g., Figure 1 B). Each plot was obtained from measurements of ΔG_{II} at three to five Gdn·HCl concentrations. Three to seven individual measurements were made at each Gdn·HCl concentration. C_{IIm}, the midpoint of the Gdn·HCl-induced unfolding transition for $I^{II}_S \leftrightarrow U^{II}_S$ is obtained from $C_{IIm} = \Delta G^*_{II(H_2O)}/m_{II}$. The linear correlation coefficients, r, of the fit of the data to a straight line are given in the next to last column. [b] The free energy differences are defined as $\Delta\Delta G^*_{II} = \Delta G^*_{II(\text{iso-2 mutant"i"})} - \Delta G^*_{II(ref)}$. $\Delta G^*_{II(ref)} = \Delta G^*_{II(iso-2)}$ for all single mutants, while $\Delta G^*_{II(ref)} = \Delta G^*_{II(N52I\ iso-2)}$ for double mutants containing the N52I stability-enhancing mutation.

Table 4: Effects of Mutations on the Rate of Absorbance-Detected Slow Folding[a]

protein	$k_f (= 1/\tau_{1a})$ (s^{-1})	$\Delta G^{\ddagger}_I$[b] (kcal mol^{-1})	$\Delta\Delta G^{\ddagger}_I$[c] (kcal mol^{-1})	$[\Delta\Delta G^*_I - \Delta\Delta G^{\ddagger}_I]$[d] (kcal mol^{-1})
iso-2	5.9×10^{-2}	18.8	0	0
N52I iso-2	13.7×10^{-2}	18.3	−0.5	+0.1 ± 0.1
P30A (N52I) iso-2	3.2×10^{-2}	19.2	+0.4	−0.2 ± 0.2
H33N iso-2	6.2×10^{-2}	18.8	0	−0.7 ± 0.1
P76G iso-2	[e]	[e]	[e]	[e]
P25G iso-2	3.9×10^{-2}	19.1	+0.3	−1.0 ± 0.4
I75M (N52I) iso-2	6.8×10^{-2}	18.7	−0.1	+2.5 ± 0.7

[a] The apparent rate of absorbance-detected slow folding. The rate constant for kinetic phase τ_{1a} (the $I^I_S \rightarrow N$ reaction) is given for 20 °C, 0.1 M sodium phosphate, pH 6, and 0 M Gdn·HCl. All rate constants, $k_f = 1/\tau_{1a}$, are for the uncatalyzed reactions measured in the absence of PPI where τ_{1a} is the time constant for the absorbance-detected slow-folding reaction. The rate constants at 0 M Gdn·HCl are obtained from the Y-axis intercept of a linear regression analysis of plots of log k_f vs Gdn·HCl. Measurements were made at three to five different Gdn·HCl concentrations between 0 and 0.7 M Gdn·HCl. Three to seven individual measurements were made at each Gdn·HCl concentration. [b] Activation free energies for absorbance-detected slow folding (the $I^I_S \rightarrow N$ reaction) obtained as $\Delta G^{\ddagger}_I = RT \ln[(k_b T/h)\tau_{1a}]$, where R is the gas constant, k_b = Boltzmann's constant, h = Planck's constant, T = 293.16 K, and τ_{1a} the time constant for absorbance-detected slow folding. Assuming errors in the uncatalyzed rate constants of about 10%, errors in $\Delta G^{\ddagger}_I$ are estimated to be less than 0.1 kcal mol^{-1}. [c] Mutation-induced changes in the activation free energy for absorbance-detected slow folding relative to iso-2 (single mutants) or N52I iso-2 (double mutants). For single point mutations, $\Delta\Delta G^{\ddagger}_I = \Delta G^{\ddagger}_{I(\text{iso-2 mutant})} - \Delta G^{\ddagger}_{I(iso-2)}$. For double mutants containing the N52I stability-enhancing mutation, $\Delta\Delta G^{\ddagger}_I = \Delta G^{\ddagger}_{I(\text{iso-2 double mutant})} - \Delta G^{\ddagger}_{I(N52I\ iso-2)}$. Errors in $\Delta\Delta G^{\ddagger}_I$ are estimated to be less than 0.1 kcal mol^{-1}. [d] The difference, $[\Delta\Delta G^*_I - \Delta\Delta G^{\ddagger}_I]$, gives the mutation-induced changes in free energy of unfolding of the transition state relative to unstructured U^I_S species in the absence of Gdn·HCl. [e] The absorbance-detected rate is not given for P76G iso-2 since phase τ_{1a} is not detected in folding of this protein (Wood et al., 1988b).

folding intermediates. Note that the free energy correlations for the absorbance-detected (I^I_S) and fluorescence-detected (I^{II}_S) intermediates fall on the same line within errors, suggesting that the two kinds of slow folding intermediates

Table 5: Effects of Mutations on the Rate of Fluorescence-Detected Slow Folding[a]

protein	$k_f (= 1/\tau_{1b})$ (s^{-1})	$\Delta G^{\ddagger}_{II}$[b] (kcal mol^{-1})	$\Delta\Delta G^{\ddagger}_{II}$[c] (kcal mol^{-1})	$[\Delta\Delta G^*_{II} - \Delta\Delta G^{\ddagger}_{II}]$[d] (kcal mol^{-1})
iso-2	8.5×10^{-2}	18.6	0	0
N52I iso-2	7.8×10^{-2}	18.7	+0.1	+0.5 ±0.4
P30A (N52I) iso-2	4.0×10^{-2}	19.1	+0.4	−1.3 ±0.4
H33N iso-2	5.8×10^{-2}	18.8	+0.2	+0.3 ±0.4
P76G iso-2	5.9×10^{-2}	18.8	+0.2	+0.3 ±0.1
P25G iso-2	5.2×10^{-2}	18.9	+0.3	−1.2 ±0.1
I75M (N52I) iso-2	11.6×10^{-2}	18.4	−0.3	+0.1 ±0.4

[a] The apparent rate of fluorescence-detected slow folding. The rate constant for kinetic phase τ_{1b} (the $I^{II}_S \rightarrow N$ reaction) is given for 20 °C, 0.1 M sodium phosphate, pH 6, and 0 M Gdn·HCl. All rate constants, $k_f = 1/\tau_{1b}$, are for the uncatalyzed reactions measured in the absence of PPI where τ_{1b} is the time constant for the fluorescence-detected slow folding reaction. The rate constants at 0 M Gdn·HCl are obtained from the Y-axis intercept of a linear regression analysis of plots of log k_f vs Gdn·HCl. Measurements were made at three to five different Gdn·HCl concentrations between 0 and 0.7 M Gdn·HCl. Three to seven individual measurements were made at each Gdn·HCl concentration. [b] Activation free energies for fluorescence-detected slow folding (the $I^{II}_S \rightarrow N$ reaction) obtained as $\Delta G^{\ddagger}_{II} = RT \ln[(k_b T/h)\tau_{1b}]$, where R is the gas constant, k_b = Boltzmann's constant, h = Planck's constant, T = 293.16 K, and τ_{1b} the time constant for fluorescence-detected slow folding. Assuming errors in the uncatalyzed rate constants of about 10%, errors in $\Delta G^{\ddagger}_{II}$ are estimated to be less than 0.1 kcal mol^{-1}. [c] Mutation-induced changes in the activation free energy for fluorescence-detected slow folding relative to iso-2 (single mutants) or N52I iso-2 (double mutants). For single point mutations, $\Delta\Delta G^{\ddagger}_{II} = \Delta G^{\ddagger}_{II(\text{iso-2 mutant})} - \Delta G^{\ddagger}_{II(iso-2)}$. For double mutants containing the N52I stability-enhancing mutation, $\Delta\Delta G^{\ddagger}_{II} = \Delta G^{\ddagger}_{II(\text{iso-2 double mutant})} - \Delta G^{\ddagger}_{II(N52I\ iso-2)}$. Errors in $\Delta\Delta G^{\ddagger}_{II}$ are estimated to be less than 0.1 kcal mol^{-1}. [d] The difference, $[\Delta\Delta G^*_{II} - \Delta\Delta G^{\ddagger}_{II}]$, gives the mutation-induced changes in free energy of unfolding of the transition state relative to unstructured U^{II}_S species.

are stabilized by common factors. The combined correlation for both types of intermediates (r = 0.961) is even better than for equilibrium stability. Despite the fact that the functional relationship between equilibrium stability and m values differs from that of the intermediate stability and the m_I or m_{II} values, there may be some common factors that stabilize both folding intermediates and the thermodynamically stable conformations. For example, an important common determinant of the m_I, m_{II}, and m values, may be the change in solvent exposure of hydrophobic surface on unfolding. The common contributors to stability of equilibrium and intermediate conformations may result in the overall correlation (r = 0.72) between stability for both equilibrium and intermediate states and the respective m, m_I, and m_{II} values.

While common factors may lead to an overall correlation, different factors may determine the mutation-induced *differences* in equilibrium stability and the stability of folding intermediates. This seems likely because of the very different functional relationship between equilibrium stability and m values compared to the dependence of the stability of the intermediates on m_I or m_{II} values. The slope of the line correlating equilibrium stability and the m value is 3.5 ± 1.1 M while that correlating the stability of the slow folding intermediates to the $m_{I,II}$ values is only 0.61 ± 0.05 M. There are also significant differences in the y-axis intercepts. The y-axis intercept is negative (intercept = −6.6 ± 3.7 kcal mol^{-1}) for the correlation between equilibrium stability and m value but is positive (intercept = +2.9 ± 0.1 kcal mol^{-1})

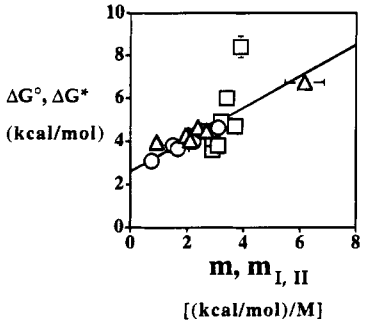

FIGURE 2: Free energy correlations for iso-2 and mutational variants of iso-2. The squares show the correlation between the equilibrium free energy of unfolding measured from Gdn·HCl-induced unfolding transitions, $\Delta G°_{U(H_2O)}$, and the guanidine hydrochloride dependence of the apparent free energy, $m = d\Delta G_U/d[\text{Gdn·HCl}]$, for iso-2 and mutational variants of iso-2. The data are taken from Table 1. The least-squares fit of the equilibrium unfolding data (the squares) to a straight line gives a slope = 3.5 ± 1.1 M, an intercept = −6.6 ± 3.7 kcal mol^{-1}, and a correlation coefficient, r = 0.82. The triangles show the correlation between the apparent free energy of unfolding ($\Delta G^*_{I(H_2O)}$) of the absorbance-detected intermediates and the guanidine hydrochloride dependence of the apparent free energy, $m_I = d\Delta G_I/d[\text{Gdn·HCl}]$. The least-squares fit to the data for the absorbance-detected intermediates to a straight line gives a slope = 0.56 ± 0.06 M, an intercept = 3.2 ± 0.2 kcal mol^{-1}, and a correlation coefficient r = 0.978. The circles show the relationship between the apparent free energy of unfolding ($\Delta G^*_{II(H_2O)}$) of the fluorescence-detected intermediates and the guanidine hydrochloride dependence of the apparent free energy, $m_{II} = d\Delta G_{II}/d[\text{Gdn·HCl}]$. The least-squares fit of the data for the fluorescence-detected intermediates to a straight line gives a slope = 0.65 ± 0.07 M, an intercept = 2.7 ± 0.2 kcal mol^{-1}, and a correlation coefficient r = 0.975. The combined least-squares fit of the data for both types of intermediates (circles and triangles) to a straight line gives a slope = 0.61 ± 0.05 M, an intercept = 2.9 ± 0.1 kcal mol^{-1}, and a correlation coefficient r = 0.961. The data for the intermediates are taken from Tables 2 and 3. The solid line is the least-squares fit of all the data (squares, circles, and triangles) to a straight line with a slope = 0.74 ± 0.17 M, an intercept = 2.6 ± 0.5 kcal mol^{-1}, and a correlation coefficient, r = 0.716. Note that the functional relationship (i.e., slope, intercept) of the conformational stability to the m_I, m_{II}, or m values is the same within errors for the entire data set as for either of the intermediates. However, there is a significantly different functional relationship (i.e., slope, intercept) of the equilibrium stability to the (equilibrium) m values. Error bars are shown for data points where the error exceeds the size of the symbols.

for the correlation between the stability of the slow folding intermediates and the m_I and m_{II} values.

Mutational Effects on Equilibrium Stability. The order of the stabilities measured by Gdn·HCl-induced unfolding and by thermal unfolding (scanning calorimetry) is in good agreement. For example, arrangement of the proteins in order of increasing T_m from thermal unfolding gives the same order as ordering the proteins on the basis of increasing C_m from Gdn·HCl-induced unfolding. The proper way to compare protein stabilities, however, is by standard free energies of unfolding. For all proteins other than P76G iso-2, N52I iso-2, and I75M, N52I iso-2, the standard free energies of unfolding obtained from Gdn·HCl-induced unfolding are in reasonably good agreement with those measured by scanning calorimetry. For P76G iso-2, I75M, N52I iso-2, and, to a lesser extent, N52I iso-2, temperature-induced unfolding (scanning calorimetry) gives a substantially smaller standard free energy of unfolding than analysis of the Gdn·HCl-induced unfolding transitions. This may be because thermal unfolding and Gdn·HCl-induced unfolding measure different transitions. For example, the thermally unfolded states for these proteins may contain residual structure which is unfolded in the Gdn·HCl-induced unfolding transitions. For P76G iso-2 in particular, the thermal-induced unfolding transition measured by absorbance is very broad and asymmetric, suggesting that temperature-induced unfolding involves significant concentrations of intermediates stable at equilibrium (Nall, 1995). In addition, the m value for Gdn·HCl-induced unfolding of N52I iso-2 is significantly larger than for iso-2. Differences in m values for denaturant-induced unfolding of closely related mutant proteins have been attributed to mutation-induced differences in structure in the unfolded states of the proteins (Shortle & Meeker, 1986, 1989). On the other hand, P30A, N52I iso-2 has a larger m value than iso-2, but the standard free energy of unfolding is the same (within errors) for scanning calorimetry and Gdn·HCl-induced transitions.

With the exception of the stability-enhancing mutation, N52I, stabilities measured by Gdn·HCl unfolding show that all the single-substitution point mutations generate proteins less stable than the parental protein from which they were derived. This is regardless of whether the stabilities are measured by standard free energies (from Gdn·HCl unfolding) or by the transition midpoints, C_m. The N52I mutation enhances the stability of iso-2 substantially (by ~3.5 kcal mol^{-1}) as does the analogous mutation in yeast iso-1 cytochrome *c* (Das et al., 1989; Hickey et al., 1991). A double mutant protein carrying the N52I stability-enhancing mutation, I75M, N52I iso-2, is also more stable than iso-2, but by substantially less than N52I iso-2. The I75M mutation is destabilizing, at least in the context of N52I iso-2, since I75M, N52I iso-2 is about 2.4 kcal mol^{-1} less stable than N52I iso-2. Another double mutant protein, P30A, N52I iso-2 is substantially less stable than N52I iso-2 (~3.7 kcal mol^{-1} less stable), but comparable in stability to iso-2. The P30A, N52I iso-2 double mutant protein illustrates a useful feature of the N52I stability-enhancing mutation in suppressing the deleterious effects of other mutations (Das et al., 1989; Hickey et al., 1991). This makes it possible to construct stable double mutant proteins in which the second mutation is at a location in the amino acid sequence where a single substitution yields a protein too unstable to study. For example, previous attempts to obtain mutations at position 30 in iso-2 in the absence of the N52I mutation have led to highly unstable proteins (Wood et al., 1988a).

Stability of Folding Intermediates. The absorbance-detected slow folding intermediates (I^I_S intermediates) are surprisingly stable (Table 2) and are comparable in stability to the equilibrium stabilities for the same proteins (Table 1). However, in comparing the stabilities of slow folding intermediates (I$_S$ states) to the stabilities of folded proteins (Table 1 vs Table 2), a small correction is necessary, since the reference states differ. Stability measurements of slow-folding intermediates, use a pure U$_S$ state as the free energy reference (U_S^I for the I_S^I intermediates; or U_S^{II} for the I_S^{II} intermediates). Measurements of the equilibrium thermodynamic stability of the N state use a mixed unfolded state consisting of U_F, U^I_S, and U^{II}_S species as the free energy reference. The equilibrium stabilities (Table 1) may be expressed relative to pure U^I_S or U^{II}_S states using the following expressions:

$$\Delta G°_{U^I_S} = \Delta G° + 0.97 \text{ kcal mol}^{-1} \qquad (9A)$$

$$\Delta G^\circ_{U^{II}_S} = \Delta G^\circ + 1.53 \text{ kcal mol}^{-1} \quad (9B)$$

Equations 9A and 9B are derived from estimates of the equilibrium populations of the U_F (73%), U^I_S (19%), and U^{II}_S (8%) species (Osterhout & Nall, 1985) in the unfolded protein. Equation 9 allows comparison of the stabilities of slow-folding intermediates to the equilibrium stability of the folded protein using the same free energy reference states (U^I_S or U^{II}_S). Using eq 9 to compare the stabilities of slow-folding intermediates to those of the N states of the folded proteins shows that most of the folded proteins are only slightly more stable (0.3−1.2 kcal mol^{-1}) than the slow-folding intermediates. This suggests that for some of the variant proteins there may be small populations of I_S intermediates present at equilibrium. N52I iso-2 is an exception with the I^I_S intermediates 5.1 kcal mol^{-1} less stable than the fully folded protein measured by Gdn·HCl-induced unfolding. It is interesting that the stability of the I^I_S intermediates (ΔG^*_I) is about the same (4−4.7 kcal mol^{-1}) for most of the proteins. Most of the m_I values are also comparable, falling in the range of 2−2.7 kcal mol^{-1} M^{-1}. The striking exception is I75M, N52I iso-2 for which I^I_S is about 2−2.7 kcal mol^{-1} more stable than for the other proteins ($\Delta G^*_I = 6.7 \pm 0.7$ kcal mol^{-1}). In addition, the m_I value for I75M, N52I iso-2 is 2−3-fold greater than for the other I^I_S intermediates. This suggests that position 75 (or the I75M mutation itself) plays an important role in stabilizing the I^I_S intermediates. This is not particularly surprising, since position 75 immediately precedes Pro76, which has been assigned to the absorbance-detected slow-folding phase (Wood et al., 1988a,b). The I^I_S intermediates for P25G iso-2 have an unusually small m_I value (= 0.9 ± 0.7 kcal mol^{-1} M^{-1}), but the small correlation coefficient for this data set ($r = 0.43$) makes interpretation of the P25G iso-2 data difficult.

The fluorescence-detected I^{II}_S intermediates are also comparable in stability to the fully folded forms of the same proteins. Once again, I75M, N52I iso-2 is exceptional with $\Delta G^*_{II} = 3.8$ kcal mol^{-1}, substantially less than the equilibrium stability of $\Delta G^\circ_{U^{II}_S} = 7.5$ kcal mol^{-1}. A comparison of ΔG^*_{II} for N52I iso-2 and I75M, N52I iso-2 shows that the I75M mutation has a slightly destabilizing effect on the I^{II}_S intermediates. This is in contrast to the strongly stabilizing effect of the same mutation on the I^I_S intermediates. Similar to the I^I_S intermediates, the m_{II} values for the I^{II}_S intermediates are comparable to or less than the corresponding m values for equilibrium unfolding, suggesting that unfolding of the intermediates is less cooperative and occurs over a wider range of denaturant concentrations than equilibrium unfolding.

Effects of Mutations on Transition States. The activation free energy barriers for the $I^I_S \rightarrow N$ reactions are all large and fall in a range from slightly over 18 kcal mol^{-1} to slightly over 19 kcal mol^{-1}. Mutations for which $\Delta\Delta G^\ddagger_I \neq 0$ affect the energetics of structural changes that occur as the I^I_S species are converted to the transition state, $[I^I_S]^\ddagger$. The sign conventions used for $\Delta\Delta G^\ddagger_I$ are such that negative values of $\Delta\Delta G^\ddagger_I$ arise for mutations which make the $I^I_S \rightarrow [I^I_S]^\ddagger$ transition easier, while positive values occur for mutations which make it more difficult to reach the transition state. Three positions, 25, 30, and 52, are identified as having significant affects on the $I^I_S \rightarrow [I^I_S]^\ddagger$ transition. The largest effect is that of the N52I mutation, which lowers the free energy barrier ($\Delta\Delta G^\ddagger_I = -0.5$ kcal mol^{-1}). The P30A mutation increases the free energy barrier ($\Delta\Delta G^\ddagger_I = +0.4$ kcal mol^{-1}), while $\Delta\Delta G^\ddagger_I = +0.3$ kcal mol^{-1} for P25G iso-2. For all proteins studied, the mutation-induced changes in the activation free energies ($\Delta\Delta G^\ddagger_I$) are very small compared to the barrier heights ($\Delta G^\ddagger_I$). This is an expected consequence of the fact that the time scale for slow folding is governed primarily by slow *cis*−*trans* isomerization of proline imide bonds: the activation free energy for *cis*−*trans* isomerization is the major contributor to the total activation free energy barrier for slow folding. Mutations affect the rates of slow folding, but only by perturbing structure within the transition state that modulates the intrinsic rate of isomerization.

The quantity $\Delta\Delta G^\ddagger_I$ (and $\Delta G^\ddagger_I$) measures free energy changes relative to the I^I_S state, a structured intermediate state. It is also useful to compare values of the difference $[\Delta\Delta G^*_I - \Delta\Delta G^\ddagger_I]$ which gives the mutation-induced changes in the unfolding free energy of the transition state relative to a (presumably) unstructured U^I_S state. The quantity $[\Delta\Delta G^*_I - \Delta\Delta G^\ddagger_I]$ identifies locations which are structured in the transition state regardless of whether the positions participate in the energetics of the $I^I_S \rightarrow [I^I_S]^\ddagger$ transition. Three locations are identified: positions 25, 33, and 75. Mutations at positions 25 and 33 (P25G iso-2, and H33N iso-2) decrease the structural stability of the transition state relative to U^I_S, while the I75M mutation enhances structural stability relative to U^I_S. Mutations at these three positions have little or no effect on the rates of absorbance-detected slow folding since the mutations alter stability of the I^I_S intermediates and the transition state $[I^I_S]^\ddagger$ in a similar manner.

Fluorescence-detected slow folding is similar in outline but differs in detail from absorbance-detected slow folding. Analogous to the $I^I_S \rightarrow N$ reactions, the activation free energy barriers for the $I^{II}_S \rightarrow N$ reactions are all large and fall in a narrow range from slightly over 18.4−19.1 kcal mol^{-1}. A comparison of the values of $\Delta\Delta G^\ddagger_{II}$ identifies three locations affecting the energetics of the $I^{II}_S \rightarrow [I^{II}_S]^\ddagger$ reaction: positions 25, 30, and 75. The mutations at positions 25 and 30 increase the activation free energy barrier, while the mutation at position 75 decreases the barrier. There are smaller, marginally significant affects for mutations at positions 33 and 76. Comparisons of values of $[\Delta\Delta G^*_{II} - \Delta\Delta G^\ddagger_{II}]$ show that positions 25 and 30 participate in structure in the transition state, $[I^{II}_S]^\ddagger$, which is melted out in the U^{II}_S species.

Stability of Intermediates as a Determinant of Structural Specificity in Folding. One view of protein folding intermediates is that they are simply "bumps" in the free energy path between the unfolded protein and thermodynamically most stable conformation, the N state. Intrinsically slow steps may act as kinetic traps to folding. By slowing down folding, the kinetic traps encourage the accumulation of high concentrations of structured (misfolded) intermediate species. In such instances, even highly populated intermediates may not be absolutely necessary for successful folding. Specific examples are the slow-folding intermediates which are formed because rapid folding is impeded by intrinsically slow processes such as proline isomerization or disulfide interchange. Do these slow-folding intermediates have any real importance, or are they simply artifacts of the kinetics of folding? We propose that slow-folding intermediates represent alternative structures to which a protein folds under appropriate conditions or as a result of changes in amino

acid sequence. Of course these alternative structures may be "native-like" and retain much of the structure of the native protein, except near critical proline residues. Slow-folding intermediates are the subject of the present study, but fast folding intermediates may also result from kinetic traps behind which alternative (intermediate) structures accumulate (Baldwin, 1995; Elove et al., 1994; Sosnick et al., 1994). Faster folding kinetically trapped intermediates may differ from slow-folding intermediates only in the depth of the free energy "bump" along the folding pathway. So what determines whether a polypeptide chain folds to one alternative structure (i.e., I_S) or another (N)? The accepted view is that a protein will fold to the conformation with the greatest equilibrium thermodynamic stability (largest $\Delta G°_U$) under the conditions of refolding. Changes in conditions and amino acid sequence can change which structure is most stable. For example iso-2 folds to a nonnative alkaline form at high pH (Nall, 1986). Moreover, folding to the alkaline conformation involves formation of an *intermediate* that has the spectral and redox properties of the *native* conformation! Thus, the native conformation appears to be a free energy "bump" along the folding pathway leading to the alkaline conformation. Sequence is important too, since some mutant variants of iso-2 fold to the alkaline form under conditions where iso-2 takes on the native conformation (Nall et al., 1989). Thus, both the refolding conditions and amino acid sequence play roles in determining which of the alternative structures, alkaline or native, is selected. Under fixed refolding conditions, some changes in sequence appear to tilt the overall free energy profile towards one alternative structure or another.

Figure 3 provides a quantitative assessment of the relative effects of several mutations on the stability of slow-folding intermediates and on the stability of the native conformation. In Figure 3A the mutation-induced change in the stability of the absorbance-detected I^I_S intermediates is plotted versus equilibrium thermodynamic stability. Points falling on the solid diagonal line have equal effects on the stability of I^I_S and N. These kinds of mutations have no effect on the preferences for folding to one conformation or another and are neutral with regard to the structural specificity of folding. Three of the mutant proteins, however, are well off the diagonal. For N52I iso-2 the stability of the N state is increased (a large positive $\Delta\Delta G°$) while the stability of the I^I_S species is only marginally affected. Thus, the N52I mutation enhances the structural specificity for folding to the N state. In contrast the P30A and the I75M mutations shift the structural specificity, at least partially, toward the I^I_S species. With P30A, N52I iso-2 the shift occurs because the N-state is much less stable while the stability of the I^I_S intermediates is unchanged. For I75M, N52I iso-2, the shift results from a decrease in the stability of the N-state combined with an increase in the stability of the I^I_S intermediates. Both P30A, N52I iso-2 and I75M, N52I iso-2 end up folding to the N-state, under the standard conditions (20 °C, 0.1 M sodium phosphate, pH 6), so the N-state remains favored over the I^I_S state. Nevertheless, Figure 3A shows that the I75M or the P30A mutation reduces the free energy difference between these two states. Figure 3B gives a similar analysis of the mutational effects on the structural preferences between the I^{II}_S state and the N state. In this case, P25G is the only (neutral) mutation which has no affect on the relative structural specificity for folding to the I^{II}_S state or the N state. As with the I^I_S species, the N52I mutation enhances the structural specificity for folding to the N state by greatly increasing the stability of the N-state while having only small effects on the stability of the I^{II}_S state. The effect of all the remaining mutations is to shift the structural specificity of folding more toward the I^{II}_S state. For P76G iso-2 and H33N iso-2 this occurs by combining modest decreases in stability of the N-state with modest increases in stability of the I^{II}_S state. For P30A, N52I iso-2

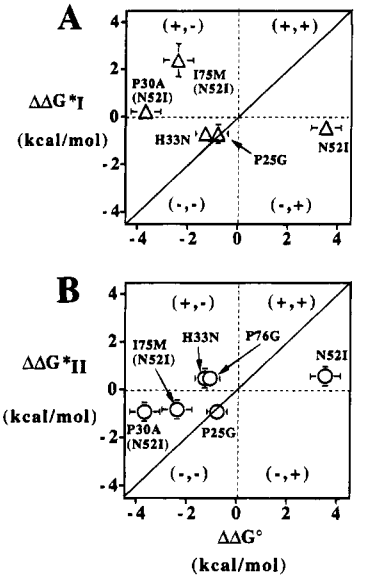

FIGURE 3: Relationship between the mutational effects on the apparent stability of slow folding intermediates and mutational effects on equilibrium thermodynamic stability. The difference free energies are defined as $\Delta\Delta G_i = \Delta G$(iso-2 mutant"i")$_i - \Delta G$(ref), where the free energy values are taken from Tables 1, 2, and 3. ΔG(ref) = ΔG(iso-2) for all single mutants, while ΔG(ref) = ΔG(N52I iso-2) for double mutants containing the N52I stability enhancing mutation. In panel A the open triangles give $\Delta\Delta G^*_{I(H_2O)}$, the mutation-induced change in the unfolding free energy for the absorbance-detected slow folding intermediates, versus $\Delta\Delta G°_{U(H_2O)}$, the mutation-induced change in the equilibrium unfolding free energy for each mutant. In panel B the open circles give $\Delta\Delta G^*_{II(H_2O)}$, the mutation-induced change in the unfolding free energy for the fluorescence-detected slow folding intermediates, versus $\Delta\Delta G°_{U(H_2O)}$, the mutation-induced change in the equilibrium unfolding free energy for each mutant. For reference, solid lines of slope = 1 are drawn for both panel A and panel B. Points falling on the line indicate that the mutation has the same effect on the stability of the intermediate and the equilibrium thermodynamic stability. Points falling above or below the line indicate that the mutation has different effects on the stability of the intermediate and equilibrium thermodynamic stability. Points falling above the horizontal dashed line indicate that the mutation has a stabilizing effect on the intermediates. Points falling below the dashed line are for mutations with a destabilizing effect on the intermediate. For equilibrium thermodynamic stability, points on the right of the vertical dashed line are for stabilizing mutations and those on the left are for destabilizing mutations. The four quadrants defined by the vertical and horizontal dashed lines are labeled according to whether mutant proteins falling in that quadrant show stabilizing (+) or destabilizing (−) effects on intermediate stability and equilibrium stability, respectively. For example, a point falling in the (+,−) quadrant indicates a mutant protein with enhanced stability of a slow-folding intermediate but decreased equilibrium thermodynamic stability. Schematic free energy profiles for the folding reactions of the mutant proteins in each of the four quadrants are given in Figure 4. All free energy differences are for 20 °C, 0 M Gdn·HCl, and 0.1 M sodium phosphate, pH 6. Error bars are shown for data points where the error exceeds the size of the symbols.

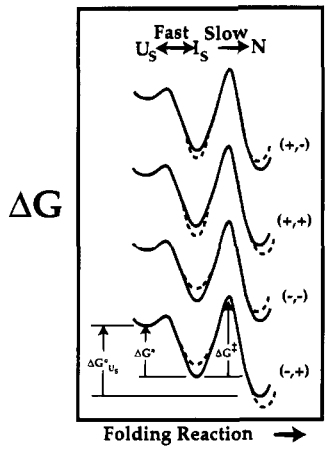

FIGURE 4: Free energy profiles for slow protein folding reactions with one stable intermediate. U_S species are PPI-accessible slow-folding species, while I_S are structured PPI-inaccessible slow-folding intermediates in which the structure blocks access of PPI to the proline residues in the intermediate. N is the native protein. The free energies measured from equilibrium unfolding ($\Delta G^\circ_{U_S}$ from eq 9), PPI catalysis of slow folding (ΔG^*), and from uncatalyzed rates of slow folding ($\Delta G^{\ddagger}$) are indicated on the free energy profile at the bottom of the figure. The curved dashed lines on the free energy profiles indicate a range of possible effects of mutations on the stability of the slow-folding intermediates, I_S, and the stability of the native protein, N. Effects of the mutations on the transition state $[I_S]^{\ddagger}$ for the $I_S \rightarrow N$ reaction are not shown but are listed in Tables 4 and 5. In drawing the profiles it is assumed that there are no effects of mutations on the stability of the U_S species, i.e., the U_S state is taken as a reference state for the free energy changes. The profiles are labeled in accord with the convention used to label the four quadrants of Figure 3. For example, the (+,−) free energy profile is that of a mutant protein with enhanced stability of I_S but decreased stability of N.

and for I75M, N52I iso-2 the mutations are, in fact, slightly destabilizing for the I^{II}_S state but are much more destabilizing for the N-state. Therefore, the overall effect is to shift the structural preferences more toward the I^{II}_S state.

Free Energy Profiles for Slow Folding. Figure 4 presents four different free energy profiles representing the four quadrants of Figure 3A,B. The profiles illustrate the various ways in which mutations can alter the structural specificity of folding by having different effects on the stability of the I_S state and the N state. The upper profile (labeled +,−) shifts the structural specificity of folding toward the I_S state and away from the N state by enhancing the stability of I_S (+) and decreasing the stability of N (−). Mutations having these combined effects fall in the upper left-hand quadrants of Figure 3A,B. Examples of mutations which stabilize I^I_S vs N are I75M and possibly P30A on folding of N52I iso-2 (Figure 3A). Mutations which stabilize I^{II}_S relative to N are H33N and P76G (Figure 3B). In contrast, the bottom profile (labeled −,+) shifts the structural specificity of folding away from the I_S state and toward the N state by decreasing the stability of I_S (−) and enhancing the stability of N (+). Such mutations fall in the lower right hand quadrant of Figure 3. The only example of this kind of effect among the mutant proteins studied is the change in stability of I^I_S relative to N observed for N52I iso-2 (Figure 3A). Mutant proteins with free energy profiles like the one second from the top in Figure 4 (labeled: +,+) have enhanced stability for both I_S (+) and N (+). When the magnitudes of the effects on I_S and N are equal, the structural specificity is unchanged. For unequal effects, the shift in the structural specificity of folding depends on whether the magnitude of the stabilizing effect is greater for I_S or for N, respectively. The only example of a (+,+) effect is the change in stability of I^{II}_S compared to N observed for N52I iso-2 (Figure 3B), where the shift in structural specificity is toward the N state. Finally, as shown in the free energy profile third down from the top in Figure 4 (labeled: −,−), the mutation can destabilize both I_S and N. When the destabilizing effects are equal for I_S and N, there is no change in the structural specificity (e.g., the effects of the H33N and P25G mutations on the I^I_S vs N states shown in Figure 3A, and the effect of the P25G mutation on the I^{II}_S vs N states in Figure 3B). Both P30A, N52I iso-2 and I75M, N52I iso-2 have (−,−) types of free energy profiles for folding of the I^{II}_S intermediates (Figure 3B). For both of these mutant proteins the shift in structural specificity is toward the I^{II}_S state, since the mutations destabilize the N state more than the I^{II}_S state.

Design of Thermodynamically Stable Forms of Folding Intermediates. Two aspects of the results suggest that it may be possible to design mutant proteins which retain the conformation of the I_S state at equilibrium. First, the stabilities measured for the I_S states are comparable to those of the N state. So only modest shifts in relative stability toward the I_S state are required. Second, mutations which bring about shifts in stability toward the I_S state relative to N appear to be common. This includes all mutant proteins which fall on the upper left side of the solid diagonal line in Figure 3: two out of five proteins in Figure 3A and four out of six proteins in Figure 3B. For example, the P30A and I75M mutations favor the I^I_S state, while P30A, H33N, I75M, and P76G all favor stabilization of the I^{II}_S state. If the effects of the mutations on shifting the structural preferences toward an I_S form are additive, then the combination of these mutations in a single polypeptide may be sufficient to create a protein that folds to I_S rather than N. Since all prolines in the N state of iso-2 contain *trans* imide bonds (Murphy et al., 1992), the criteria for success in creating a stable I_S state are clear. A protein for which I_S is the thermodynamically stable conformation will (1) have two high amplitude folding phases of opposite sign, a fast phase ($U_F \rightarrow N$) followed by a slow phase ($N \rightarrow I_S$), and (2) contain at least one proline with a *cis* imide bond.

CONCLUSIONS

Catalysis of slow folding by prolyl isomerase has been shown to provide a means of measuring the structural stability of slow folding intermediates relative to PPI-accessible forms of the refolding protein. These intermediates may be kinetically trapped "native-like" structures in many respects but will contain nonnative *cis*-prolines. Measurements with mutant variants of the parental protein show that mutations often have different effects on the stability of intermediates and the equilibrium stability of the fully folded protein. This allows identification of mutations which enhance stability of intermediates relative to the native state and suggests an empirical means of constructing mutant proteins that fold to thermodynamically stable structures closely related to the structure of slow folding intermediates.

ACKNOWLEDGMENT

Drs. Jun Liu, C. T. Walsh, and G. L. Verdine are thanked for providing strains used to overexpress human PPI (cy-

clophilin) in *E. coli*. Dr. H. B. Bächinger is thanked for providing several suggestions on the purification of PPI. We thank Dr. Susan Weintraub for electrospray ion mass spectrometry which was used to verify the integrity of the primary structure of mutant proteins used in this work. We also thank C. S. Raman for his help with the calorimeter and various other instruments and for installing and maintaining much of the software used for data analysis.

REFERENCES

Bachinger, H. P. (1987) *J. Biol. Chem. 262*, 17144−17148.
Baldwin, R. L. (1995) *J. Biomol. NMR 5*, 103−109.
Becktel, W. J., & Schellman, J. A. (1987) *Biopolymers 26*, 1859−1877.
Brandts, J. F., Halvorson, H. R., & Brennan, M. (1975) *Biochemistry 14*, 4953−4963.
Das, G., Hickey, D. R., McLendon, D., McLendon, G., & Sherman, F. (1989) *Proc. Natl. Acad. Sci. U.S.A. 86*, 496−499.
Elove, G. A., Bhuyan, A. K., & Roder, H. (1994) *Biochemistry 33*, 6925−6935.
Fischer, G., & Bang, H. (1985) *Biochim. Biophys. Acta 828*, 39−42.
Garel, J. R., & Baldwin, R. L. (1973) *Proc. Natl. Acad. Sci. U.S.A. 70*, 3347−51.
Glasstone, S., Laidler, K. J., & Eyring, H. (1941) *The Theory of Rate Processes*, McGraw-Hill Book Co., New York.
Guillemette, J. G., Barker, P. D., Eltis, L. D., Lo, T. P., Smith, M., Brayer, G. D., & Mauk, A. G. (1994) *Biochimie 76*, 592−604.
Harrison, R. K., & Stein, R. L. (1990) *Biochemistry 29*, 3813−3816.
Hickey, D. R., Berghuis, A. M., Lafond, G., Jaeger, J. A., Cardillo, T. S., McLendon, D., Das, G., Sherman, F., Brayer, G. D., & McLendon, G. (1991) *J. Biol. Chem. 266*, 11686−11694.
Inglis, S. C., Guillemette, J. G., Johnson, J. A., & Smith, M. (1991) *Protein Eng. 4*, 569−574.
Kelley, R. F., & Richards, F. M. (1987) *Biochemistry 26*, 6765−6774.
Kiefhaber, T., Quaas, R., Hahn, U., & Schmid, F. X. (1990) *Biochemistry 29*, 3053−3061.
Lang, K., Schmid, F. X., & Fischer, G. (1987) *Nature 329*, 268−270.
Lattman, E. E., & Rose, G. D. (1993) *Proc. Natl. Acad. Sci. U.S.A. 90*, 439−41.
Liggins, J. R., Sherman, F., Mathews, A. J., & Nall, B. T. (1994) *Biochemistry 33*, 9209−9219.
Mayo, S. L., & Baldwin, R. L. (1993) *Science 262*, 873−876.
Montgomery, D. L., Leung, D. W., Smith, M., Shalit, P., Faye, G., & Hall, B. D. (1980) *Proc. Natl. Acad. Sci. U.S.A. 77*, 541−545.
Murphy, M. E., Nall, B. T., & Brayer, G. D. (1992) *J. Mol. Biol. 227*, 160−176.
Nall, B. T. (1983) *Biochemistry 22*, 1423−1429.
Nall, B. T. (1986) *Biochemistry 25*, 2974−2978.
Nall, B. T. (1995) in *Cytochrome c. A Multidisciplinary Approach* (Scott, R. A., & Mauk, A. G., Eds.) University Science, Mill Valley, CA.
Nall, B. T., & Landers, T. A. (1981) *Biochemistry 20*, 5403−5411.
Nall, B. T., Osterhout, J. J., & Ramdas, L. (1988) *Biochemistry 27*, 7310−7314.
Nall, B. T., Zuniga, E. H., White, T. B., Wood, L. C., & Ramdas, L. (1989) *Biochemistry 28*, 9834−9839.
Osterhout, J. J., & Nall, B. T. (1985) *Biochemistry 24*, 7999−8005.
Pace, C. N. (1986) *Methods Enzymol. 131*, 266−280.
Pace, C. N. (1990a) *Trends Biochem. Sci. 15*, 14−17.
Pace, C. N. (1990b) *Trends Biotechnol. 8*, 93−98.
Santoro, M. M., & Bolen, D. W. (1988) *Biochemistry 27*, 8063−8068.
Schellman, J. A. (1978) *Biopolymers 17*, 1305−1322.
Schellman, J. A. (1987a) *Biopolymers 26*, 549−559.
Schellman, J. A. (1987b) *Annu. Rev. Biophys. Biophys. Chem. 16*, 115−137.
Schmid, F. X. (1993) *Annu. Rev. Biophys. Biomol. Struct. 22*, 123−143.
Schmid, F. X., & Baldwin, R. L. (1978) *Proc. Natl. Acad. Sci. U.S.A. 75*, 4764−4768.
Schmid, F. X., Mayr, L. M., Mucke, M., & Schonbrunner, E. R. (1993) *Adv. Protein Chem. 44*, 25−66.
Schonbrunner, E. R., Mayer, S., Tropschug, M., Fischer, G., Takahashi, N., & Schmid, F. X. (1991) *J. Biol. Chem. 266*, 3630−3635.
Shortle, D., & Meeker, A. K. (1986) *Proteins 1*, 81−89.
Shortle, D., & Meeker, A. K. (1989) *Biochemistry 28*, 936−944.
Sosnick, T. R., Mayne, L., Hiller, R., & Englander, S. W. (1994) *Nature Struct. Biol. 1*, 149−156.
Veeraraghavan, S., & Nall, B. T. (1994) *Biochemistry 33*, 687−692.
Wood, L. C., Muthukrishnan, K., White, T. B., Ramdas, L., & Nall, B. T. (1988a) *Biochemistry 27*, 8554−8561.
Wood, L. C., White, T. B., Ramdas, L., & Nall, B. T. (1988b) *Biochemistry 27*, 8562−8568.
Zuniga, E. H., & Nall, B. T. (1983) *Biochemistry 22*, 1430−1437.

BI951212P